

# Planar cyclotron motion in unidirectional superlattices defined by strong magnetic and electric fields: Traces of classical orbits in the energy spectrum

S. D. M. Zwerschke, A. Manolescu<sup>†</sup>, and R. R. Gerhardts

*Max-Planck-Institut für Festkörperforschung, Heisenbergstraße 1, D-70569 Stuttgart, Germany*

<sup>†</sup>*Institutul Național de Fizica Materialelor, C.P. MG-7 București-Măgurele, România*

We compare the quantum and the classical description of the two-dimensional motion of electrons subjected to a perpendicular magnetic field and a one-dimensional lateral superlattice defined by spatially periodic magnetic and electric fields of large amplitudes. We explain in detail the complicated energy spectra, consisting of superimposed branches of strong and of weak dispersion, by the correspondence between the respective eigenstates and the “channeled” and “drifting” orbits of the classical description.

## I. INTRODUCTION

In the last decade there has been a constant interest in the transport properties of the periodically modulated two dimensional electron gas (2DEG). In particular, in the presence of a lateral modulation of a one-dimensional character the resistivity may be strongly anisotropic, which essentially reflects the anisotropy of the electronic states. Two types of modulations can be achieved in the experimental devices: electrostatic potential modulations<sup>1–4</sup> and, more recently, magnetic field modulations.<sup>5–8</sup> Weak modulations of both types lead already to pronounced magnetoresistance effects in the presence of an average magnetic field  $B_0$  applied perpendicular to the 2DEG. These effects occur at low and intermediate  $B_0$  values, well below the magnetic quantum regime where Shubnikov-de Haas oscillations appear. At very small values of  $B_0$  a pronounced positive magnetoresistance is observed, followed at intermediate  $B_0$  values by the “Weiss oscillations” due to commensurability effects. Both effects are adequately understood within a classical transport calculation based on Boltzmann’s equation, and can be traced back to the predominance of different types of classical trajectories.<sup>9–11</sup>

The positive magnetoresistance is understood as caused by “channeled orbits” which exist if the modulation is sufficiently strong or, equivalently, the average magnetic field is sufficiently small. For electric modulation they occur near the minima of the modulation potential (“open” orbits<sup>10</sup>), and for magnetic modulation near the lines of vanishing total magnetic field (“snake” orbits<sup>12</sup>). They are always confined within a single period of the modulation, which we choose in  $x$  direction. They are wavy trajectories allowing for fast motion of electrons with velocities within small angles around the direction of translational invariance ( $y$  direction). These

channeled orbits occur in addition to the “drifting orbits”, which are self-intersecting trajectories with loops (along each of which the direction of the velocity changes by  $2\pi$ ), so that usually a low drift velocity in  $y$  direction results. For sufficiently small  $B_0$ , drifting orbits may extend over many periods of the modulation. At sufficiently large  $B_0$  (sufficiently small modulation amplitudes) only the drifting orbits survive. The “Weiss oscillations” manifest a commensurability effect depending on the ratio of the extent of drifting orbits (at the Fermi energy) and the modulation period. With increasing modulation strength, the positive magnetoresistance becomes more pronounced and extends to larger  $B_0$  values, suppressing progressively the low- $B_0$  Weiss oscillations.<sup>10</sup> This effect is well understood within the classical calculation<sup>11</sup>, if both types of trajectories are adequately included, and it has recently also been obtained by a quantum calculation for a strong modulation<sup>13</sup>.

A qualitatively new type of magnetoresistance effect has recently been observed by Ye *et al.*<sup>14</sup> on samples with an extremely strong magnetic modulation. Samples with a surface array of ferromagnetic micro-strips were measured in tilted magnetic fields, so that the applied magnetic field had a large component parallel to the surface, producing a large magnetization of the ferromagnetic strips, while only the small perpendicular component determined the average magnetic field  $B_0$  in the 2DEG. In this way a huge positive magnetoresistance with superimposed Shubnikov-de Haas like oscillations was obtained at low values of the average magnetic field, at which no magnetic quantum effects should be expected for weak modulation.<sup>14</sup> It rather seems that the quantum oscillations are induced by the large-amplitude periodic magnetic modulation field. Such conditions require a quantum transport theory and, as a first step, the understanding of the quantum electronic states of a 2DEG with a strong magnetic modulation. This is the motivation of the present work.

Channeled and drifting quantum states in linearly varying magnetic field are already discussed by other authors.<sup>12,15</sup> The Schrödinger equation for periodic magnetic fields alternating in sign, has been solved previously, but only for the case when the average field is zero<sup>16</sup>. In the present paper we shall study the quantum electronic states in strong periodic magnetic fields with a non-vanishing average, and compare it with the case of a strong electric modulation. In both situations, rather complicated energy spectra are obtained, with striking

qualitative similarities and quantitative differences. For the case of strong electric modulation, such a complicated energy spectrum has recently been published<sup>13</sup>, but without an attempt of an explanation. We will demonstrate in this paper that a close comparison with classical motion leads to a detailed and intuitive understanding of these spectra and the corresponding eigenstates.

In Sec. II we start with some general remarks on the relation between quantum and classical description of the 2D electron motion in 1D lateral superlattices, and we introduce suitable reduced units. In Sec. III we focus on the effect of a simple harmonic magnetic modulation of arbitrary strength. In Sec. IV we include an electric modulation, which requires a somewhat different analytical procedure. The inclusion of electric modulation seems also necessary from the experimental point of view, since the ferromagnetic strips on the sample surface introduce a periodic stress field in the sample, which acts as an electric modulation on the 2DEG. Finally, in Sec. V we summarize the essential features derived in the paper and extend the discussion beyond the model of simple harmonic modulations.

Some of the present results have been recently published in a preliminary form.<sup>17</sup>

## II. GENERAL REMARKS

We consider a (non-interacting) 2DES in the  $x$ - $y$  plane subjected to a magnetic field with  $z$  component  $B_z(x) = B_0 + B_m(x)$  and an electrostatic field in  $x$  direction leading to a potential energy  $U(x)$ . Our aim is a close comparison of the classical and the quantum description of the electron motion (in terms of orbits and wavefunctions, respectively) in such fields, especially in the case that  $U(x)$  and  $B_m(x)$  are periodic in  $x$  with the same period  $a$  and vanishing average values.

To evidence the translation invariance in  $y$  direction in the (either classical or quantum) Hamiltonian

$$H = \frac{1}{2m} (\mathbf{p} + e\mathbf{A})^2 + U, \quad (1)$$

we describe  $B_z(x)$  by an  $x$ -dependent vector potential  $\mathbf{A}(x) = A(x) \mathbf{e}_y$  with  $A(x) = xB_0 + A_m(x)$  and  $A_m(x) = \int_0^x dx' B_m(x')$ . Then  $y$  is a cyclic variable and the canonical momentum  $p_y$  is conserved, and one obtains an (one-dimensional) effective Hamiltonian  $H(X_0) = p_x^2/2m + V(x; X_0)$ . For  $B_0 \neq 0$ , the effective potential can be written

$$V(x; X_0) = \frac{m}{2} \omega_0^2 \left( x - X_0 + \frac{A_m(x)}{B_0} \right)^2 + U(x), \quad (2)$$

where  $X_0 = -p_y/eB_0$  is the center coordinate of the effective potential and  $\omega_0 = eB_0/m$  is the cyclotron frequency, both in the absence of modulation.

In the quantum description, the reduction to a one-dimensional problem is achieved by the product ansatz

$\Psi_{n,X_0}(x, y) = L_y^{-1/2} \exp(ip_y y/\hbar) \psi_{n,X_0}(x)$  for the energy eigenfunctions, where  $L_y$  is a normalization length, and the discrete quantum number  $n = 0, 1, 2, \dots$  counts the nodes of the reduced wavefunction  $\psi_{n,X_0}(x)$ . If  $U(x)$  and  $A_m(x)$  are bounded, the  $\psi_{n,X_0}(x)$  drop Gaussian-like for  $|x| \rightarrow \infty$ , and for a fixed value of the quasi-continuous quantum number  $X_0$  the energy spectrum  $E_n(X_0)$  is discrete.

In the classical description, we use the equation  $mv_y = p_y + eA(x)$ , which may also be derived directly from Newton's equation, to eliminate the velocity  $v_y$ . The effective motion in  $x$  direction is determined by  $H(X_0) = E$ . Similar to the wavefunctions, the orbits for given constants of motion,  $X_0$  and  $E$ , are bounded in  $x$  direction, however the energy  $E$  is a continuous variable. For a given  $E = E_F$ , each position  $x$  (with  $U(x) < E_F$ ) is the turning point of two orbits which are characterized by the center coordinates<sup>11</sup>

$$X_0^\pm(x) = x + \frac{A_m(x)}{B_0} \pm R_0 \sqrt{1 - \frac{U(x)}{E_F}}, \quad (3)$$

obtained from  $H(X_0) = E_F$  for  $v_x = p_x/m = 0$ . Here  $R_0 = v_F/\omega_0$  is the cyclotron radius of electrons moving with energy  $E_F = mv_F^2/2$  in the magnetic field  $B_0$ . For given  $E_F$  and  $X_0$ , orbits exist in intervals in which  $X_0^-(x) \leq X_0 \leq X_0^+(x)$  holds. This allows a convenient classification of the possible orbits at fixed energy  $E_F$  and for varying  $X_0$ .<sup>11</sup> Of course, the same classification can also be done by directly investigating the effective potential. This may be preferred if one is interested in orbits at different energies but the same  $X_0$ .

The calculation of the orbits is a simple textbook problem, but must in general be done numerically. In accordance with the translational symmetry of the problem, we will in the following not distinguish orbits which differ only by a rigid shift in  $y$  direction. If an electron is at time  $t_i$  at position  $(x_i, y_i)$  on an orbit characterized by the constants of motion  $E_F$  and  $X_0$ , with turning points  $x_l$  and  $x_r$  ( $x_l < x_i < x_r$ ), it moves towards one of the turning points so that at time

$$t(x; X_0, E_F) = t_i + \int_{x_i}^x \frac{dx'}{|v_x(x'; X_0, E_F)|} \quad (4)$$

it is at position  $(x, y(x; X_0, E_F))$ , with

$$y(x; X_0, E_F) = y_i + \int_{x_i}^x \frac{v_y(x'; X_0)}{v_x(x'; X_0, E_F)} dx', \quad (5)$$

where  $|v_x(x; X_0, E_F)| = v_F \sqrt{1 - V(x; X_0)/E_F} = \omega_0 \sqrt{[X_0^+(x) - X_0][X_0 - X_0^-(x)]}$  and  $v_y(x; X_0) = (\omega_0/2)[X_0^+(x) + X_0^-(x) - 2X_0]$ . If at one of the turning points  $x_l$  or  $x_r$ , where  $v_x(x; X_0, E_F) = 0$ , the derivative  $\partial V(x; X_0)/\partial x$  vanishes, we call this turning point and this orbit "critical". At critical turning points the integrals (4) and (5) diverge, so that the critical orbits there asymptotically approach straight lines

parallel to the  $y$  axis. For non-critical orbits the integrals (4) and (5) converge as  $x$  approaches the turning points, and the total orbit can be composed out of right-running ( $v_x > 0$ ) and left-running ( $v_x < 0$ ) pieces with finite traverse time  $T(X_0, E_F) = \int_{x_l}^{x_r} dx/|v_x(x; X_0, E_F)|$ . The probability density of finding the electron at position  $x$  is  $W(x; X_0, E_F) = 1/[T(X_0, E_F)|v_x(x; X_0, E_F)|]$ . This is the classical analog to  $|\psi_{n, X_0}(x)|^2$ .

If  $U(x) = U(x + a)$  and  $B_m(x) = B_m(x + a)$  are periodic with period  $a$ , as we will assume in the following, the effective potential, Eq. (2), has the symmetry  $V(x + a; X_0 + a) = V(x; X_0)$ . As a consequence, the energy spectrum is also periodic,  $E_n(X_0 + a) = E_n(X_0)$ , and can be restricted to the “first Brillouin zone”  $0 \leq X_0 \leq a$ . The eigenfunctions can be taken to satisfy  $\psi_{n, X_0+a}(x) = \psi_{n, X_0}(x - a)$ . The corresponding classical symmetry is that an orbit characterized by  $E_F$  and  $X_0 + a$  differs from that characterized by  $E_F$  and  $X_0$  only by a rigid shift of amount  $a$  in  $x$  direction.

The dispersion of the energy bands  $E_n(X_0)$  implies a group velocity in  $y$  direction,

$$\langle n, X_0 | v_y | n, X_0 \rangle = -\frac{1}{m\omega_0} \frac{dE_n(X_0)}{dX_0}, \quad (6)$$

which is the expectation value of the velocity operator in the energy eigenstate  $\psi_{n, X_0}$ . It is the quantum equivalent to the classical drift velocity, i.e. the average velocity (in  $y$  direction) along the corresponding classical orbit. The drift velocity in  $x$  direction vanishes, since the orbits are bounded in  $x$  direction.

### A. Suitable units

For an economic comparison of classical and quantum aspects it is important to use suitable length and energy units, which are meaningful for both the quantum description and the classical limit. Doing so, we will see that the classical features depend on fewer scaled parameters than the quantum ones. To be specific but still rather general, we assume in the following periodic modulations of the form  $B_m(x) = B_m^0 b(Kx)$  and  $U(x) = V_0 u(Kx)$  for the magnetic and the electric modulation, respectively, where  $b(\xi)$  and  $u(\xi)$  are dimensionless periodic functions with period  $2\pi$  and vanishing average values. Thus  $B_m(x)$  and  $U(x)$  have the same period  $a = 2\pi/K$ , but may have different shapes and phases. In the numerical examples we will use for both  $b(\xi)$  and  $u(\xi)$  simple cosines, eventually with a phase shift.

The average magnetic field  $B_0$  sets, with the magnetic length  $l_0 = \sqrt{\hbar/(m\omega_0)}$  and the cyclotron energy  $\hbar\omega_0$ , both a length and an energy scale, which are useful for quantum calculations, but have no meaning for the classical motion. For the discussion of commensurability effects, such as the Weiss oscillations, the cyclotron orbits must be compared with the period  $a$  of the modulation.

Therefore  $a$  is a natural choice for the lengths unit. The choice of a suitable energy unit is motivated as follows.

Classically,  $B_0$  determines only the cyclotron frequency  $\omega_0$ , and one needs an independent length  $l$  to define an energy scale  $V_{\text{mag}} = m\omega_0^2 l^2/2$ . Using  $l$  as length unit, we may define dimensionless variables  $\xi = x/l$  and  $\xi_0 = X_0/l$ . The effective potential, Eq. (2), then can be written as  $V(x; X_0) = V_{\text{mag}} \tilde{v}(\xi; \xi_0)$  with

$$\tilde{v}(\xi; \xi_0) = [\xi - \xi_0 + s a(Kl\xi)/Kl]^2 + w u(Kl\xi), \quad (7)$$

where  $s = B_m^0/B_0$ ,  $a(\xi) = \int_0^\xi d\zeta' b(\zeta')$ , and  $w = V_0/V_{\text{mag}}$ . In the quantum description, the kinetic energy operator  $-(\hbar^2/2m)d^2/dx^2 = -E_l d^2/d\xi^2$ , introduces a new energy scale  $E_l = \hbar^2/(2ml^2)$ , which has no classical analog. Introducing the energy ratio  $\alpha = E_l/V_{\text{mag}}$ , we write the effective Schrödinger equation as

$$\left[ -\alpha \frac{d^2}{d\xi^2} + \tilde{v}(\xi; \xi_0) - \tilde{\varepsilon}_n(\xi_0) \right] \tilde{\psi}_{n, \xi_0}(\xi) = 0, \quad (8)$$

with  $\tilde{\varepsilon}_n(\xi_0) = E_n(X_0)/V_{\text{mag}}$  and  $\tilde{\psi}_{n, \xi_0}(\xi) = \sqrt{l} \psi_{n, X_0}(x)$ .

If we would take  $l = l_0$ , we had  $V_{\text{mag}} = E_l = \hbar\omega_0/2$  and thus simply  $\alpha = 1$ . The effective potential Eq. (7) would then depend on the constant of motion  $\xi_0$  and, in addition, on three dimensionless model parameters,  $s$ ,  $w$ , and  $Kl_0$ . To specify an eigenstate or, in the classical description, a trajectory, one further needs an energy value  $\tilde{\varepsilon}$  as a second constant of motion. A description that, for fixed constants of motion, needs *three* parameters to specify the effective potential and, furthermore, relies on  $l_0$  and  $\hbar\omega_0$ , which have no meaning in classical mechanics, is rather clumsy and not acceptable.

Instead we take  $l = 1/K$  and, therefore,  $V_{\text{mag}} = V_{\text{cyc}}$ , where  $V_{\text{cyc}} = m\omega_0^2/(2K^2)$  is the energy of a classical cyclotron orbit of radius  $1/K$  in the homogeneous magnetic field  $B_0$ . Now the effective potential Eq. (7) depends only on the *two* dimensionless modulation strengths  $s$  and  $w = V_0/V_{\text{cyc}}$ , which both are well defined within the classical approach. Also the constants of motion,  $\xi_0 = KX_0$  and  $\tilde{\varepsilon} = E/V_{\text{cyc}} = (KR_0)^2$ , including the dimensionless version of Eq. (3),

$$\xi_0^\pm(\xi) = \xi + s a(\xi) \pm \sqrt{\tilde{\varepsilon} - w u(\xi)}, \quad (9)$$

remain meaningful in the classical limit. This choice of units will also be very useful for a systematic discussion of the quantum mechanical energy spectra. Quantum mechanics enters the effective Schrödinger equation (8) only via the parameter  $\alpha = (l_0 K)^4$ , which scales the kinetic energy. It determines the only true quantum aspect of the spectrum, namely the spacing of the energy levels  $\tilde{\varepsilon}_n(\xi_0)$ . We will see in Sec. IIIB that all the essential structural features of the energy spectrum, e.g. the complicated back-folded structure due to the coexistence of “channeled” and “drifting” states, are determined solely by the “classical” parameters  $s$  and  $w$ . The density of the quantized levels  $\tilde{\varepsilon}_n(\xi_0)$ , on the other hand, increases with increasing ratio  $a/l_0$ .

As a simple example one may consider the well known case of a weak electric or magnetic cosine modulation, which leads to modified Landau bands of oscillatory width.<sup>2,4,18,19</sup> The band width assumes minima near the “flat band” energies  $E_\lambda^\pm = m(\omega_0 a)^2(\lambda \pm 1/4)/8$ , with “+” (“−”) for magnetic (electric) modulation and  $\lambda = 1, 2, \dots$ . These flat band energies are distinct multiples of our energy unit  $V_{\text{cyc}}$ , and occur at  $\varepsilon_\lambda^\pm = \pi^2(\lambda \pm 1/4)$ , independent of the special values of the model parameters  $B_0$  and  $a$ . The level spacing, on the other hand, is of the order  $\hbar\omega_0$  and depends in our units on  $\hbar\omega_0/V_{\text{cyc}} = 2l_0^2 K^2 = 2\sqrt{\alpha}$ .

### III. MAGNETIC COSINE MODULATION

We first consider a pure magnetic modulation,  $U(x) \equiv 0$ ,  $B_m(x) = B_m^0 b(Kx)$ , so that the effective potential Eq. (7) becomes

$$V(\xi; \xi_0) = V_{\text{cyc}}[\xi - \xi_0 + s a(\xi)]^2. \quad (10)$$

For  $s = 0$  one obtains the well known Landau levels and the Landau oscillator wave functions,  $f_{nX_0}(x)$ . We use the set  $f_{nX_0}$  as the basis of our Hilbert space in order to obtain numerical solutions for  $s \neq 0$ , by numerical diagonalization of  $H(X_0)$ . The electron effective mass is that of GaAs,  $m = 0.067m_0$ . We further assume spin degeneracy. For the numerical parameters chosen here the size of the basis will vary between 150-300 Landau levels.

Before discussing the numerical results we summarize some properties of the effective potential and of Eq. (9), which now reduces to

$$\xi_0^\pm(\xi) = \xi + s a(\xi) \pm KR_0. \quad (11)$$

For a fixed  $\xi_0$  the local extrema of the effective potential, given by  $\partial V(\xi, \xi_0)/\partial \xi = 0$ , are the points where the total magnetic field is zero, i. e. the roots of

$$1 + s b(\xi) = 0, \quad (12)$$

and the points where the effective potential is zero, i. e. the roots of

$$\xi - \xi_0 + s a(\xi) = 0. \quad (13)$$

An important aspect for the following discussion is that the roots of the first kind, Eq.(12), if existent, are independent of  $\xi_0$ , while those of the second kind, Eq.(13), do depend on  $\xi_0$ . We will see that orbits with  $\xi$  values near roots of the first kind are channeled, while those with  $\xi$  values near roots of the second kind are drifting orbits. The analytic dependence of the effective potential on the relevant position coordinate  $\xi$  is determined by the modulation strength  $s$ . Therefore the number of its possible zeroes, the classification of orbits and the energy spectrum depend critically on the parameter  $s$ . To demonstrate this, we choose in the following examples  $b(\xi) = \cos \xi$ , and consequently  $a(\xi) = \sin \xi$ .

#### A. Weak modulation, $s \leq 1$

For  $s < 1$ , the effective potential has exactly one minimum of the second kind for each value  $\xi_0$ , which is due to the confinement by the average magnetic field. The functions  $\xi_0^\pm(\xi)$  in equation (11) have no extrema. For each value  $\xi_0$  they determine exactly one orbit, which is a drifting cyclotron orbit. By this we mean a self-intersecting orbit consisting of loops along each of which the azimuth angle in velocity space,  $\varphi = \arctan(v_y/v_x)$  increases by  $2\pi$ . A typical example is illustrated in Fig. 1 for  $s = 0.5$ ,  $\xi_0 = \pi/2$  (i.e.  $X_0 = a/4$ ), and two energy values  $E_F$ . Figure 1(a) shows the effective potential. For a given energy  $E = E_F$  (horizontal line) a classical orbit exists where  $V(\xi; \xi_0) \leq E_F$ . Figure 1(b) shows the location of the turning points as the crossing points of the horizontal line  $\xi_0 = \pi/2$  with the functions  $\xi_0^\pm(\xi)$ . The corresponding drifting orbit exists in the interval with  $\xi_0^-(\xi) \leq \xi_0 \leq \xi_0^+(\xi)$ . The orbits in real space are illustrated in Fig. 1(c). In Fig. 2 we plot the corresponding quantities for  $s = 0.5$  and  $\xi_0 = \pi$  (i.e.  $X_0 = a/2$ ). In this case the effective potential is symmetric with respect to the center coordinate  $X_0$ . As a consequence, the orbits are closed and their drift velocity in  $y$  direction is zero.

For small energies,  $E_F/V_{\text{cyc}} = (KR_0)^2 < \pi^2$  (i.e.  $2R_0 < a$ ), the extents of the orbits in  $x$  direction are smaller than a modulation period and essentially determined by the local values of the total magnetic field. At high energies,  $E_F/V_{\text{cyc}} \gg 1$ , the orbits extend over several periods of the modulation and the extent of an orbit, i.e., the width of the effective potential valley at the corresponding energy, is determined by the cyclotron radius in the average magnetic field ( $x_r - x_l \approx 2R_0$ ).

In Fig. 3(a) we display the first 50 energy bands  $E_{n\xi_0}$  calculated from the (first 150) original, degenerated Landau levels, for  $s=0.5$ . The level spacing of the lowest energy bands is seen to follow the local value of the total magnetic field, Fig. 3(b). This is expected from the local approximation  $E_{n\xi_0} \approx (n + 1/2)\hbar eB(\xi_0)/m$ , which is valid if the extent of the wavefunctions  $\psi_{n,X_0}(x)$  is smaller than the modulation period. With our energy unit  $V_{\text{cyc}}$  the apparent level spacing of energies which are independent of the period  $a$  becomes proportional to  $\sqrt{\alpha}$ . For example, if the local approximation  $E_{n\xi_0} \approx (n + 1/2)\hbar\omega(\xi_0)$  holds for  $E_{n\xi_0} < 4V_{\text{cyc}}$ , as in Fig. 3(a), this implies that it holds for  $n + 1/2 < 4V_{\text{cyc}}/[\hbar\omega(\xi_0)] = 2[\omega_0/\omega(\xi_0)]/\sqrt{\alpha}$ . Thus, the number of bands which are well described by the local approximation increases quadratically with increasing modulation period  $a$ .

The local approximation fails at higher energies when the width of the wavefunctions becomes larger than the period of the modulation, and the structure of the energy spectrum changes. Indeed it is well known from the limit of very weak magnetic modulation,  $s \ll 1$ , that in contrast to this local approximation the bands become flat at the energies  $E_\lambda/V_{\text{cyc}} = \pi^2(\lambda + 1/4)$ , for

$\lambda = 1, 2, \dots$ <sup>18,19,6</sup> These flat band conditions are the quantum equivalents to the classical commensurability conditions leading to the Weiss oscillations in magnetotransport, and do not change their positions in a plot like Fig. 3(a), even if we change the modulation period. A larger modulation period  $a$  just leads to a higher density of the energy bands.

In Fig. 3(c) we plot for  $\xi_0 = \pi/2$  the effective potential and the square of the energy eigenfunctions for the energy values considered in Fig. 1. Width and location of the wavefunctions in the effective potential is in close agreement with that of the corresponding classical orbits. In Fig. 3(d) we plot the corresponding quantities for the symmetric situation  $\xi_0 = \pi$ , to be compared with Fig. 2. These wavefunctions belong to (relative) extrema of the energy bands, and thus have zero group velocity, in agreement with the zero drift velocity of the corresponding classical orbits. The wavefunctions in Fig. 3(c) belong to finite energy dispersion and describe motion in the positive ( $n=3$ ) and the negative ( $n=43$ )  $y$  direction, respectively, in agreement with the corresponding classical orbits in Fig. 1. For large quantum numbers  $n$  and weak modulation the group velocities can be shown to reduce quantitatively to the drift velocities of the corresponding classical orbits.

In Fig. 4 we consider the “critical” situation  $s = 1$ . The derivatives  $\xi_0^{\pm'}(\xi_{ex}) = 0$  and  $\xi_0^{\pm''}(\xi_{ex}) = 0$  vanish for  $\xi_{ex} = (2p+1)\pi$  ( $p$  integer), i.e. for the positions where the magnetic field vanishes, Eq.(12). For all values of  $\xi_0$  the effective potential (7) becomes flat at these points  $\xi_{ex}$  (see Fig. 4(c)). The classical situation is as for  $s < 1$  with the exception that for  $\xi_0 = \xi_{ex} \pm KR_0$  there are “critical” orbits which asymptotically approach straight lines parallel to the  $y$  axis on their left (for  $+$ ) or their right (for  $-$ ) side, where  $B(x) = 0$ . The dashed lines plotted over the energy spectrum of Fig. 4(a) show the evolution of the flat regions of the effective potential with  $\xi_0$ , i.e. the parabolas resulting from  $V(\xi_{ex}; \xi_0)$  with  $p = 0$  and  $p = \pm 1$ . In the first Brillouin zone these lines are seen as the back-folding of the lowest parabola centered on  $\xi_{ex}$  with  $p = 0$ , and they are an indication of a kind of a free electron motion along the lines where the magnetic field is zero. Close to these parabolas the energy bands have large dispersion near inflexion points, and the energy separation between adjacent bands is minimum. Similar features have been obtained in the energy spectra for single magnetic wells by Peeters and Matulis.<sup>20</sup> In other words, such states experience a weak effective magnetic field, due to the constant effective potential over a substantial spatial region. The wavefunctions corresponding to states with large energy dispersion have large amplitudes at the positions of flat effective potential (vanishing total magnetic field). This is demonstrated for two selected states [ $(n=43, \xi_0=3.18)$  and  $(n=5, \xi_0=0.50)$ ] in Fig. 4(b), together with the probability distributions of the corresponding classical orbits. The effective potentials together with the corresponding classical orbits are plotted in Fig. 4(c). The trajectory corresponding to the

state ( $n=5, \xi_0=0.50$ ) is close to a critical orbit with a critical right turning point. This leads to an enhanced probability density near that point, which is also reflected in the quantum mechanical probability density.

We will see that for slightly stronger modulation a new type of nearly free motion occurs with energies close to the parabolas  $V(\xi_{ex}; \xi_0)$  in the energy spectrum.

## B. Strong modulation, $s > 1$

For  $s > 1$ ,  $\xi_0^{\pm'}(\xi) = 0$  at  $a(\xi) \equiv \cos \xi = -1/s$ , and  $\xi_0^{\pm}(\xi)$  has extrema at the following positions:

$$\begin{aligned} \text{minima : } \xi_{min}^{(p)} &= (2p+1)\pi + \delta, \\ \text{maxima : } \xi_{max}^{(p)} &= (2p+1)\pi - \delta, \end{aligned} \quad (14)$$

where  $p$  is an integer and  $\delta = \arctan \sqrt{s^2 - 1}$ . The values at these extrema are

$$\begin{aligned} \xi_0^{\pm}(\xi_{min}^{(p)}) &= (2p+1)\pi - g(s) \pm KR_0 \\ \xi_0^{\pm}(\xi_{max}^{(p)}) &= (2p+1)\pi + g(s) \pm KR_0, \end{aligned} \quad (15)$$

where

$$g(s) = \sqrt{s^2 - 1} - \arctan \sqrt{s^2 - 1} > 0. \quad (16)$$

The effective potential  $V(\xi; \xi_0)$  has extrema of the first kind, Eq. (12), at the same positions. The extrema with values  $V(\xi_{min}^{(p)}; \xi_0) = V_{cyc}[(2p+1)\pi - g(s) - \xi_0]^2$  are minima if  $(2p+1)\pi > \xi_0$ , and maxima otherwise, and those with values  $V(\xi_{max}^{(p)}; \xi_0) = V_{cyc}[(2p+1)\pi + g(s) - \xi_0]^2$  are maxima if  $(2p+1)\pi > \xi_0$ , and minima otherwise.

### 1. Classical approach

The number of zeroes of  $\xi_0^{\pm}(\xi) - \xi_0$  depends on both  $s$  and  $\xi_0$ . If  $g(s) < \pi$ ,  $\xi_0^{\pm}(\xi) - \xi_0$  has at most three zeroes. If  $\xi_0 = \xi_0^{\pm}(\hat{\xi})$  for any  $\hat{\xi}$  satisfying  $\xi_{max}^{(p)} < \hat{\xi} < \xi_{min}^{(p)}$ , i.e. if  $(2p+1)\pi - g(s) < \xi_0 \mp KR_0 < (2p+1)\pi + g(s)$ ,  $\xi_0^{\pm}(\xi) - \xi_0$  has three zeroes. The same argument holds for Eq. (13), i.e. the effective potential has three zeroes. For  $(2p-1)\pi + g(s) < \xi_0 \mp KR_0 < (2p+1)\pi - g(s)$ , on the other hand, there exists only a single zero.

In Fig. 5 we show, for  $s = 2$  [i.e.  $g(s)=0.685$ ], an example where the effective potential has a single zero near  $\xi/2\pi = 0.1$ , so that for sufficiently low energy only a single drifting orbit exists. The number and the type of the possible orbits depend on the energy. At the highest energy shown in Fig. 5(a) two orbits exist (solid lines in Fig. 5(d)). There is a drifting cyclotron orbit extending over more than two periods of the modulation, with the left turning point on  $\xi_0^+(\xi)$  (uppermost curve in Fig. 5(c)) near  $\xi/2\pi = -1.1$ , and the right turning point on  $\xi_0^-(\xi)$  (bottom curve in Fig. 5(c)) near  $\xi/2\pi = 1.3$ . Near the relative minimum of  $\xi_0^-(\xi)$  close to  $\xi/2\pi = 1.7$ , which

corresponds to a relative minimum of the effective potential (thick dashed line in Fig. 5(a)), there exists a “channeled orbit” moving in positive  $y$  direction. We define channeled orbits as trajectories which have both turning points either on  $\xi_0^+(\xi)$  or on  $\xi_0^-(\xi)$ , in contrast to the drifting orbits with one turning point on  $\xi_0^+(\xi)$  and the other on  $\xi_0^-(\xi)$ . In contrast to the self-intersecting drifting orbits, the channeled orbits are always confined to less than a single modulation period, and they move without self-intersections in a relatively narrow interval of angles around the positive or the negative  $y$  direction [see Fig. 5(d)]. Note that the curvature of the trajectories changes sign at the positions where the total magnetic field vanishes, see Fig. 5(b).

If we lower the energy to  $E/V_{\text{cyc}} = 40$ , we arrive in Fig. 5 at a situation where only a single drifting orbit exists (dashed lines). In general, the extent in  $\xi$  direction of the drifting orbits decreases with decreasing energy. At the lowest energy indicated in Fig. 5 (lowest dotted line in (a) and innermost lines in (c)), we have again a drifting orbit near  $\xi/2\pi = 0.1$  and a channeled orbit around  $\xi/2\pi = 0.6$ . At this low energy, the extent of the drifting orbit is considerably smaller than the modulation period.

In Fig. 6 we show, for the same modulation strength,  $s = 2$ , a situation,  $\xi_0 = \pi$ , where the effective potential has three zeroes, as is emphasized in the inset of Fig. 6(a). These zeroes are separated by two shallow maxima. If a (positive)  $E$  value below these maxima is chosen, one finds three narrow drifting cyclotron orbits located around the zeroes of the effective potential (solid lines). For higher energies one may find either one drifting and two channeled orbits (dotted lines) or a single drifting orbit (e.g. for  $0.5 < E/V_{\text{cyc}} < 30$ , not indicated in the figure). Actually the “drifting” orbits located around  $\xi = \pi$  have zero drift velocity due to symmetry reasons.

In summary, for  $0 < g(s) < \pi$  we find for given values of the constants of motion,  $\xi_0$  and  $E$ , at least one and at most three orbits. For larger values of  $s = B_m^0/B_0$ , more orbits may exist for a given pair of  $\xi_0$  and  $E$  values. A careful analysis of the extrema of the functions  $\xi_0^\pm(\xi)$  shows, e.g., that for  $\pi < g(s) < 2\pi$  between three and five orbits belong to the same pair of  $\xi_0$  and  $E$ . We will come back to this case below.

Apparently the plots of the effective potential  $V(\xi; \xi_0)$  are very useful to see which orbits are possible for a fixed value of the center coordinate  $\xi_0$  and different energies. Channeled orbits exist in side valleys near relative minima of  $V(\xi; \xi_0)$ . If, on the other hand, the energy of the motion is given, the plots of the locations of turning points  $\xi_0^\pm(\xi)$  is very useful to classify the possible orbits for different values of  $\xi_0$ . Channeled orbits exist near relative minima of  $\xi_0^-(\xi)$  and relative maxima of  $\xi_0^+(\xi)$ .

## 2. Quantum calculation

The energy spectra become more complicated in the case  $s > 1$ , Fig. 7 and 8. Regions of different character can be distinguished in these spectra. Areas, where the energy bands are nearly parallel lines with low dispersion (region I), alternate with regions, where steep bands with large dispersion seem to cross bands with weak dispersion (region II). In fact the energy bands never cross each other and the apparent intersections are anti-crossing points with exponentially small gaps.

The boundaries of these regions are given by classical values only. If the energy is scaled by the classical cyclotron energy  $V_{\text{cyc}}$ , for fixed modulation strength  $s$  the regions II are surrounded by the parabolas  $E = V(\xi_{\text{min}}^{(p)}; \xi_0)$  and  $E = V(\xi_{\text{max}}^{(p)}; \xi_0)$  which, for  $|p| \leq 2$ , are indicated by dashed lines in the spectra. For any fixed  $\xi_0$  such a pair of parabolas gives the minimum and the maximum value of a certain side valley of the effective potential  $V(\xi; \xi_0)$  (extrema of the first kind, see Eq. (12)). The energy interval in between these values indicates the depth of that valley, i.e. an energy range in which classically channeled orbits exist, in addition to the drifting orbits.

In Fig. 7(b) the effective potential is plotted for the symmetric case  $\xi_0 = \pi$  (dotted line), corresponding to the classical situation described in Fig. 6. Also shown are the states for  $n = 0$  (lower solid line) and for  $n = 20$  (upper solid line) and  $n = 22$  (upper dashed line). Apparently, state  $n = 20$  corresponds to a classical drifting orbit, whereas  $n = 22$  is the symmetric superposition of two states corresponding to channeled orbits in the side valleys. The latter has practically the same energy as the corresponding antisymmetric superposition ( $n = 21$ ), which is not shown. On the scale of Fig. 7(a), all states  $n = 20, 21$ , and  $22$  seem to have the same energy,  $E/V_{\text{cyc}} \approx 38$ . The states  $n = 21$  and  $22$  are hybridizations of states belonging to the branches with high energy dispersion and opposite sign of the group velocity

$$\langle v_y \rangle = -\frac{K}{m\omega_0} \frac{dE_{n\xi_0}}{d\xi_0}. \quad (17)$$

Figure 7(c) shows the effective potential for the asymmetric case  $\xi_0/2\pi = 0.2$ , corresponding to the classical situation described in Fig. 5. Here we show six states, the ground state  $n = 0$  located near the zero of the effective potential, the two “channeled” states “bound” in the potential valley around  $\xi/2\pi = 0.6$ , the extended “drifting” state  $n = 25$  near  $E = 40V_{\text{cyc}}$ , the extended state  $n = 44$ , and the localized “channeled” state  $n = 45$ . The energies of all these states are indicated in Fig. 7(a). The states which extend over more than a period of the modulation belong to weakly dispersive energy bands and correspond to the classical drifting orbits. The states belonging to the energy branches with strong dispersion have large amplitudes in side valleys of the effective potential and vanish practically outside these valleys. They correspond

to classical channeled orbits. The apparent number of nodes of the large-amplitude parts of these “channeled” states increases with energy as if they were truly bound states in these narrow valleys. Note, however, that the wave functions of channeled states still have  $n$  nodes, but the corresponding oscillations are not observable at the scale of the figure. Outside the valleys, the maxima in between the nodes are a few orders of magnitude smaller than the main peaks inside the valleys.

The number of quantized states within a given valley of the effective potential depends on the average magnetic field and the period of the magnetic modulation, even if the parameters  $V_{\text{cyc}}$  and  $s$  are fixed. In Fig.7 the period  $a$ , or the field  $B_0$ , is too small to have states quantized in the low-energy triple minimum of the effective potential for the symmetric case of Fig.7(b) (see also Fig.6). To investigate this situation, we show in Fig.8(a) a denser spectrum for the same modulations strength  $s = 2$ . In Fig.8(b) the spectrum near  $\xi_0 = \pi$  is enlarged. Five energy values are indicated, and in Fig.8(c) the corresponding (squares of the) wavefunctions are plotted for the states  $n = 0, 2, 3, 4$ , and  $5$ , together with the effective potential. The antisymmetric state  $n = 1$ , which is nearly degenerate with  $n = 2$ , is not shown. This demonstrates that all the classical features have their quantum analog, provided the model parameters (here  $\alpha$ ) are suitably chosen.

For the magnetic cosine modulation, the depth of the valleys of the effective potential,

$$|V(\xi_{\text{max}}^{(p)}; \xi_0) - V(\xi_{\text{min}}^{(p)}; \xi_0)|/V_{\text{cyc}} = 4g(s)|(2p+1)\pi - \xi_0|, \quad (18)$$

increases with the energy (i.e. with  $|p|$  for fixed  $\xi_0$ ), and thus more and more channeled states appear at higher energies. For sufficiently high energies the strips with channeled states in the energy spectra may thus extend over the whole Brillouin zone. This will also happen for sufficiently large  $s$ . The energy dispersion of the channeled states depends strongly, nearly quadratically, on  $\xi_0$  according to Eq.(10), which expresses the nearly free motion of the electrons on channeled orbits in  $y$  direction.

For  $s > 1$  and  $g(s) < \pi$ , the area of the regions II of the spectrum increases with increasing  $s$ , and the area of the regions I shrinks accordingly. For  $g(s) = \pi$ , one has  $V(\xi_{\text{min}}^{(p)}; \xi_0) = V(\xi_{\text{max}}^{(p-1)}; \xi_0)$  and the corresponding parabolas coincide, leaving no room for regions I. If the modulation is so large that  $g(s) \geq \pi$ , drifting and channeled states coexist everywhere in the spectrum. In Fig. 9 we have chosen  $s = 5$ , corresponding to  $g(s) = 3.53$ . Close to the edges of the Brillouin zone, e.g. for  $\xi_0/2\pi = 0.016$ , Fig. 9(c), we can identify channeled, e.g.  $n = 22$  and  $n = 16$ , and drifting states, e.g.  $n = 19$ . But now these drifting states are relatively narrow, confined in local minima of the effective potential and not in the wide potential well centered around  $\xi_0$ , which is given by the confinement due to the average

magnetic field. This case is already known from the discussion of Fig. 6. The local minimum of the effective potential at  $\xi = 0$  is a minimum of the second kind, with vanishing potential. Consequently, these drifting states are similar to weakly perturbed Landau levels with energy gaps  $\hbar e B(\xi_0)/m$ , as can be observed by a careful look at Fig. 9(a). In the center of the Brillouin zone say for  $\xi_0/2\pi = 0.493$ , Fig. 9(d), the effective potential has three zeroes of the second kind (see Eq.(13)) near  $\xi = \xi_0$ . We therefore can find similar narrow drifting states, like  $n = 5$  and  $n = 6$ , but also wide drifting states at higher energies, like  $n = 17$  and channeled states in local minima of first kind, like  $n = 7$ . As in the classical picture, the velocity of these narrow drifting states is in general lower than that of the channeled states.

#### IV. MIXED HARMONIC MODULATIONS

For sufficiently strong mixed electric and magnetic modulations one expects a similar situation as for the strong magnetic modulation, with a coexistence of channeled and drifting orbits, and their quantum analogs. In the presence of an electric modulation, we have no explicit analytic expressions for the minima of the effective potential, Eq. (7), not even for simply harmonic modulations. Nevertheless, a qualitative understanding of the classical and the corresponding quantum mechanical motion is possible. For a given constant of motion  $\xi_0$  the effective potential has side valleys with possible channeled orbits, if  $\partial V(\xi; \xi_0)/\partial \xi = 0$  has more than one solution  $\xi$ . This is the case, if the function

$$\xi_0(\xi) = \xi + s a(\xi) - \frac{w}{2} \frac{u'(\xi)}{1 + s b(\xi)}, \quad (19)$$

with  $w = V_0/V_{\text{cyc}}$ , assumes the value  $\xi_0(\xi) = \xi_0$  at more than one  $\xi$  value. At such  $\xi$  values the effective potential has extrema with the values

$$V(\xi; \xi_0(\xi))/V_{\text{cyc}} = w u(\xi) + \left[ \frac{w}{2} \frac{u'(\xi)}{1 + s b(\xi)} \right]^2. \quad (20)$$

To be specific, we choose for the following  $b(\xi) = \cos \xi$ ,  $a(\xi) = \sin \xi$  and  $u(\xi) = \cos(\xi + \varphi_s)$ .

Apparently, Eqs. (19) and (20) provide a parametric representation of the possible relative extrema of the effective potential in the energy-versus- $\xi_0$  diagram, similar to the dashed lines in Figs. 7 and 8 which define the regions II where “channeled” states coexist with “drifting” ones. Due to the symmetries  $\xi_0(\xi + 2\pi) = \xi_0(\xi) + 2\pi$  and  $V(\xi + 2\pi; \xi_0(\xi + 2\pi)) = V(\xi; \xi_0(\xi))$ , it is sufficient to consider only one period  $0 \leq \xi \leq 2\pi$  of the parameter  $\xi$ , provided the  $\xi_0(\xi)$  values are back-folded into the first Brillouin zone.

For strong magnetic modulation ( $s > 1$ ) the denominators in Eqs. (19) and (20) lead to poles. Then the

regions of type II extend to arbitrary high energies, similar to the case of pure magnetic modulation. A qualitatively different behavior is obtained for weak magnetic, but arbitrarily strong electric modulation, since then the denominators of Eqs. (19) and (20) remain positive (for  $s < 1$ ). Consequently, for given values of  $w$ ,  $s$ , and  $\varphi_s$  the possible values of  $V(\xi; \xi_0(\xi))$ , Eq. (20), are bound and channeled orbits can exist only below a certain energy.

### A. Pure electric modulation

As a particularly simple example we consider a pure electric cosine modulation,  $s = 0$ ,  $\varphi_s = 0$ . For weak modulation ( $w < 2$ ) the function  $\xi_0(\xi)$  of Eq. (19) has a unique inverse, i.e. the effective potential  $V(\xi; \xi_0)$  has for all values of  $\xi_0$  only a single extremum, namely the absolute minimum, and no “channeled” states should be expected. The energy spectra for this weak-modulation limit are well known<sup>2,3,13</sup> and will not be reproduced here. Apart from a phase shift, they look similar to Fig. 3(a) but with flat bands near  $E/V_{\text{cyc}} = \pi^2(\lambda - 1/4)$ , for  $\lambda = 1, 2, \dots$

The corresponding classical trajectories at sufficiently high energies are drifting cyclotron orbits. At very low energies,  $E < V_0 = wV_{\text{cyc}}$ , a peculiarity occurs, since then the classical trajectories are captured within a single valley of the electric potential, with turning points given by Eq. (9) in the interval  $\xi_c \leq \xi \leq 2\pi - \xi_c$  (modulo  $2\pi$ ) with  $\xi_c = \arccos(E/V_0) > 0$ . For  $\xi_0$  values in the interval  $\xi_c < \xi_0 < 2\pi - \xi_c$  these trajectories are self-intersecting drifting orbits, whereas for  $\xi_0 < \xi_c$  and  $\xi_0 > 2\pi - \xi_c$  there exist channeled orbits with  $v_y > 0$  and  $v_y < 0$ , respectively. The orbit with  $\xi_0 = \xi_c$  approaches the left turning point at  $\xi = \xi_c$  with a tangent parallel to the  $x$  axis, and that with  $\xi_0 = 2\pi - \xi_c$  does the same at the right turning point  $\xi = 2\pi - \xi_c$ . This peculiar low-energy behavior is, of course, not restricted to the weak modulation limit, but occurs always when the trajectories are captured in a minimum of the electric potential, i.e. for  $E < V_0$ . It is demonstrated in Fig. 10(b), and will not be discussed further.

If the electric modulation is strong enough,  $w > 2$ , the function  $\xi_0(\xi) = \xi - (w/2)\sin\xi$ , Eq. (19), has extrema at  $\xi_+ = \arccos(2/w) > 0$  and  $\xi_- = -\xi_+$  (modulo  $2\pi$ ) with values  $\xi_0(\xi_{\pm}) = \mp g(w/2)$ , where  $g(s)$  is defined by Eq. (16). Then, for  $|\xi_0| \leq g(w/2)$  the equation  $\xi_0(\xi) = \xi_0$  has three solutions  $\xi$  in the interval  $|\xi| < \pi$ , which are local extrema of the effective potential with values

$$V(\xi; \xi_0(\xi))/V_{\text{cyc}} = 1 + (w/2)^2 - [1 - (w/2)\cos\xi]^2. \quad (21)$$

In order to find in the energy spectra the regions II corresponding to side valleys of the effective potential, one may proceed as follows. One plots in the extended zone scheme  $V(\xi; \xi_0(\xi))$  versus  $\xi_0(\xi)$ , starting at  $\xi = -\pi$ , where  $\xi_0(\xi) = -\pi$  and  $V(\xi; \xi_0(\xi)) = -V_0$ . With increasing  $\xi$ , also  $\xi_0(\xi)$  and  $V(\xi; \xi_0(\xi))$  increase and reach at

$\xi = \xi_-$  their maximum values  $g(w/2)$  and  $V_{\text{cyc}}(1 + w^2/4)$ , respectively. As  $\xi$  increases from  $\xi = \xi_-$  to  $\xi = 0$ ,  $\xi_0(\xi)$  and  $V(\xi; \xi_0(\xi))$  decrease towards the values 0 and  $V_0$ , respectively. Increasing  $\xi$  from 0 to  $\pi$  leads to the mirror image of the described trace with respect to  $\xi_0 = 0$ :  $\xi_0(\xi) = -\xi_0(-\xi)$  and  $V(\xi; \xi_0(\xi)) = V(-\xi; \xi_0(-\xi))$ . Finally these four line segments have to be folded back into the “first” Brillouin zone  $0 \leq \xi_0 \leq 2\pi$  to obtain the absolute minimum of the effective potential as a function of  $\xi_0$  and the boundaries of the regions II. In contrast to the strong magnetic modulation, these regions become narrower with increasing energy and end at  $\xi_0 = \pm g(w/2)$  (modulo  $2\pi$ ) with energy  $E/V_{\text{cyc}} = 1 + w^2/4$ . For  $g(w/2) > \pi$  the back-folding leads to an overlap of different branches of the region II, that is the coexistence of back and forth running “channeled” states with “drifting” states in the same area of the  $E$ - $\xi_0$  diagram. Figure 10 shows for a typical example the quantum mechanical energy spectrum together with the boundaries of region II obtained in this manner. The “very complicated” energy spectrum obtained recently by Shi and Szeto<sup>13</sup> for strong electric modulation is thus explained by the coexistence of channeled and drifting states.

In previous work<sup>10,11</sup> it was pointed out that, for given modulation period  $a$  and strength  $V_0$  and given energy  $E = E_F$ , channeled orbits can exist only if the magnetic field  $B_0$  is smaller than a critical field  $B_{\text{crit}}$ . Solving  $E_F/V_{\text{cyc}} = 1 + w^2/4$  for  $E_F > V_0 = wV_{\text{cyc}}$  and  $w > 2$  with respect to the magnetic field, one obtains the known result<sup>11</sup>

$$B_{\text{crit}} = \frac{2\pi V_0}{eav_F} \left[ \frac{2}{1 + \sqrt{1 - (V_0/E_F)^2}} \right]^{1/2}. \quad (22)$$

### B. Weak magnetic modulation

If a magnetic modulation is added to an electric one, very complicated interference effects may result. Only if the phase shift  $\varphi_s$  is zero or  $\pi$ , the resulting energy spectrum will be symmetric in  $\xi_0$ . Even in that case, the distribution of channeled states (regions II) in the  $E$ - $\xi_0$  diagram may become rather complicated, especially at low energies. For the mixed case channeled states may occur even if the modulation parameters  $w$  and  $s$  are not large enough to produce them for the pure electric and the pure magnetic modulation of these strengths. For weak magnetic modulation,  $0 < s < 1$ , and arbitrary strength of the electric modulation, channeled states can exist only below a certain energy, as in the pure electric modulation case.

For arbitrary phase shift  $\varphi_s$  the energy spectrum may be so asymmetric that in a certain energy range only channeled orbits exist which carry current in one (say the positive  $y$ -) direction, but no channeled orbits carrying current in the opposite direction. Such a situation is



presented in Fig. 11. The regions II, where channeled and drifting states coexist, is again calculated from Eqs. (19) and (20), i.e. from purely classical arguments.

If a 2DEG is subjected to such an asymmetric mixed modulation, it may happen that in the thermal equilibrium the channeled states carry a finite current. Of course, this current must be compensated by a corresponding opposite current carried by the drifting states.

For large magnetic modulation,  $s > 1$ , and arbitrary electric modulation, the magnetic modulation dominates the energy spectra at large energies. The regions II with channeled states become more and more important, as can be seen from the pole structure of Eqs. (19) and (20). For very weak electric modulation, the results reduce to those of the pure magnetic modulation, apart from some peculiarities at very low energies, where additional regions of channeled orbits may exist.

In magnetically modulated systems prepared by deposition of magnetic micro-strips there is always an induced electric modulation due to the interface stress between the ferromagnets and the semiconductor.<sup>6</sup> The phase shift with respect to the magnetic modulation occurs when the external magnetic field is tilted.<sup>21</sup> Nevertheless, in the known experimental situations the stress potential amplitude is presumably much weaker than our bare potential.

## V. SUMMARY AND DISCUSSION

We have discussed in detail the quantum electronic states and energy spectra  $E_n(X_0)$  of a 2DEG in strong one-dimensional magnetic and electric superlattices, and in a non-vanishing average external magnetic field. By comparing the quantum results with the corresponding characteristics of the classical motion, we achieved a detailed and intuitive understanding of the energy spectra and eigenstates. We found that the complicated parts of the energy spectra (“regions II”), where branches with strong dispersion coexist with those of low dispersion, coincide with the areas in the  $E - X_0$  diagram in which classically “channeled” orbits exist.

For a systematic investigation of the possible energy spectra and eigen states, and of the corresponding types of classical trajectories, it is useful to exploit the scaling properties of the Hamiltonian. Then it is not necessary to vary independently all the basic model parameters, i.e. the strengths  $B_m^0$  and  $V_0$  of magnetic and electric modulation, the modulation period  $a$ , and the average magnetic field  $B_0$ . If one uses suitable units for energy and length,  $V_{\text{cyc}}$  and  $a/2\pi$ , respectively, one obtains the same classical results and the same gross features of the energy spectra (the same position of the regions II), if one changes the *four* parameters  $B_m^0$ ,  $V_0$ ,  $a$ , and  $B_0$  in such a manner that the *two* reduced modulation strengths  $s = B_m^0/B_0$  and  $w = V_0/V_{\text{cyc}}$  remain constant. For different parameter sets with the same values of  $s$  and  $w$ ,

only the density of the energy bands is different in the plot of  $E_n(X_0)/V_{\text{cyc}}$  versus  $KX_0$ , not its overall appearance. This is illustrated by Figs. 7(a) and 8(a), for which the regions II coincide. The reason for this behaviour is that, in these energy and length units, the effective potential is invariant under the scaling transformation  $B_m^0 \rightarrow \gamma B_m^0$ ,  $B_0 \rightarrow \gamma B_0$ ,  $a \rightarrow \lambda a$  and  $V_0 \rightarrow \gamma^2 \lambda^2 V_0$ , for arbitrary positive  $\gamma$  and  $\lambda$ . To leave the quantum result exactly unchanged under a change of the four model parameters, one has to keep  $\alpha = (l_0 K)^4$  also unchanged. This is because only with the restriction  $\lambda = 1/\sqrt{\gamma}$  the kinetic energy operator is also independent of the scaling parameter  $\gamma$  [see Eq. (8)]. Thus, in the suitable units, the exact quantum result depends only on *three* independent parameters instead of *four*, and the characteristic classical features depend only on *two*.

There is a close correspondence between the quantum states belonging to strong-dispersion branches of the energy spectrum and the classical channeled orbits. These orbits occur near lines of vanishing total magnetic field or near minima of the electric modulation potential and are restricted to individual side valleys of the effective potential. They are always restricted to a part of a single modulation period in  $x$  direction and represent a fast motion along (wavy) lines without self-intersections in positive or negative  $y$  direction. The corresponding quantum states are also essentially confined to the same space region and belong to energy branches with strong dispersion. At a given value of the constant of motion  $X_0$ , channeled orbits exist in energy intervals bounded by adjacent relative minima and maxima of the effective potential, defining bottom and top of the corresponding side valley. Plotting these classically defined extrema versus  $X_0$ , one obtains the boundaries of the regions II of the quantum energy spectrum. Classically, for each channeled orbit there exists a “drifting” orbit with the same constants of motion  $X_0$  and  $E$ . These drifting orbits are self-intersecting trajectories which, for sufficiently large energy, extend over more than one modulation period in  $x$  direction and drift slowly in  $y$  direction. The corresponding quantum states belong to low-dispersion branches of the energy spectrum. Quantum mechanically, the channeled states do not appear at exactly the same energies as the drifting states, and they usually have a larger energy spacing than the latter, since they are confined to a narrower effective potential well.

We have demonstrated these features by model calculations based on simple harmonic modulation fields. Qualitatively the obtained results and the methods to derive them can easily be extended to more general modulation fields, containing higher harmonics. This will be necessary, if the distance of the 2DEG from the sample surface is not much larger than the period of the surface structure creating the modulation.<sup>21</sup> Anharmonic effective modulation potentials may also result from non-linear screening effects, even if the bare modulation potential is harmonic.<sup>22,23</sup>

We have also performed several additional calculations

and consistency checks which are not documented in the main text. E.g., we have checked the equivalence of classical drift velocity and quantum group velocity beyond the analytically accessible case of very weak modulation fields. For some examples with strong modulation, we evaluated the quantum mechanical group velocity along several energy bands  $E_n(X_0)$  and compared the result with the drift velocity of the corresponding classical trajectories with the same energy and  $X_0$  values. For most parts of the bands the two velocities agreed perfectly. A systematic deviation was observed only in parameter regimes where the classical trajectories are close to critical orbits, which have no quantum analog. Near the critical orbits the modulus of the classical drift velocity increases rather rapidly, whereas the quantum mechanical group velocity shows no anomaly.

We have also extended the band structure calculations to very strong magnetic modulation ( $B_m^0/B_0 = 20$ ). While at high energies a complicated superposition of bands with steep and with flat dispersions, similar to that in Fig. 9(a), was obtained, the bands at low energies tend to cluster into groups separated by relatively large gaps. The low-energy part of the spectrum was already reminiscent of the spectrum for vanishing average magnetic field, where one obtains a one-dimensional Bloch energy spectrum for each value of  $p_y = -eB_0X_0$ .<sup>16</sup>

Concerning previous and forthcoming transport calculations, we conclude from the close correspondence of the quantum and the classical approach, that at weak average magnetic fields the classical calculations are appropriate, provided the modulation fields are not too strong. For the very strong magnetic modulation mentioned in the introduction, it may however happen, that the energy level spacing of “channeled orbits” exceeds the thermal energy  $k_B T$  in a regime where  $\hbar\omega_0 \ll k_B T$ . Then we would expect modulation induced quantum effects in the positive-magnetoresistance regime at low  $B_0$ .

## ACKNOWLEDGMENTS

We thank D. Pfannkuche for critical reading of the manuscript. This work was supported by the German Bundesministerium für Bildung und Forschung (BMBF), Grant No. 01BM622. One of us (A.M.) is grateful to the Max-Planck-Institut für Festkörperforschung, Stuttgart, for support and hospitality.

- <sup>2</sup> R. R. Gerhardtts, D. Weiss, and K. v. Klitzing, Phys. Rev. Lett. **62**, 1173 (1989).
- <sup>3</sup> R. W. Winkler, J. P. Kotthaus, and K. Ploog, Phys. Rev. Lett. **62**, 1177 (1989).
- <sup>4</sup> C. Zhang and R. R. Gerhardtts, Phys. Rev. B **41**, 12850 (1990).
- <sup>5</sup> H. A. Carmona *et al.*, Phys. Rev. Lett. **74**, 3009 (1995).
- <sup>6</sup> P. D. Ye *et al.*, Phys. Rev. Lett. **74**, 3013 (1995).
- <sup>7</sup> S. Izawa, S. Katsumoto, A. Endo, and Y. Iye, J. Phys. Soc. Japan **64**, 706 (1995).
- <sup>8</sup> P. D. Ye, D. Weiss, R. R. Gerhardtts, and H. Nickel, J. Appl. Phys. **81**, 5444 (1997), proceedings of the 41-st Annual Conference on Magnetism and Magnetic Materials, Atlanta 1996, and other papers therein.
- <sup>9</sup> C. W. J. Beenakker, Phys. Rev. Lett. **62**, 2020 (1989).
- <sup>10</sup> P. H. Beton *et al.*, Phys. Rev. B **42**, 9229 (1990).
- <sup>11</sup> R. Menne and R. R. Gerhardtts, Phys. Rev. B **57**, 1707 (1998).
- <sup>12</sup> J. E. Müller, Phys. Rev. Lett. **68**, 385 (1992).
- <sup>13</sup> Q. W. Shi and K. Y. Szeto, Phys. Rev. B **53**, 12990 (1996).
- <sup>14</sup> P. D. Ye *et al.*, Physica B **249-251**, 330 (1998).
- <sup>15</sup> E. Hofstetter, J. M. C. Taylor, and A. MacKinnon, Phys. Rev. B **53**, 4676 (1996).
- <sup>16</sup> I. S. Ibrahim and F. M. Peeters, Phys. Rev. B **52**, 17321 (1995).
- <sup>17</sup> A. Manolescu *et al.*, Physica B **256-258**, 375 (1998).
- <sup>18</sup> P. Vasilopoulos and F. M. Peeters, Superlatt. Microstruct. **7**, 393 (1990).
- <sup>19</sup> F. M. Peeters and P. Vasilopoulos, Phys. Rev. B **47**, 1466 (1993).
- <sup>20</sup> F. M. Peeters and A. Matulis, Phys. Rev. B **48**, 15166 (1993).
- <sup>21</sup> R. R. Gerhardtts, Phys. Rev. B **53**, 11064 (1996).
- <sup>22</sup> U. Gossmann, A. Manolescu, and R. R. Gerhardtts, Phys. Rev. B **57**, 1680 (1998).
- <sup>23</sup> A. Manolescu and R. R. Gerhardtts, Phys. Rev. B **56**, 9707 (1997).

FIG. 1. (a): Effective potential  $V(\xi; \xi_0)$  for magnetic cosine modulation with  $s = B_m^0/B_0 = 0.5$  and  $\xi_0/2\pi = 1/4$ . For a given energy  $E_F/V_{\text{cyc}} = (KR_0)^2$  (horizontal lines) classical orbits exist where  $V(\xi; \xi_0) \leq E_F$ . Solid line  $E_F = 17.6V_{\text{cyc}}$ , dotted line  $E_F = 1.18V_{\text{cyc}}$ . (b): Locations of turning points  $\xi_0^\pm(\xi)$  for the  $E_F$  values indicated in (a), same coding. Orbits with energy  $E_F$  and  $\xi_0$  exist in an interval with  $\xi_0^-(\xi) \leq \xi_0 \leq \xi_0^+(\xi)$ . (c): Corresponding orbits in  $xy$ -space, three cycles are shown each, the sense of motion is from filled to open dot.

FIG. 2. As Fig. 1, but  $\xi_0/2\pi = 1/2$ . The effective potential is symmetric and therefore the guiding center of these drifting orbits does not drift in (c).

<sup>1</sup> D. Weiss, K. v. Klitzing, K. Ploog, and G. Weimann, Europhys. Lett. **8**, 179 (1989), see also in *High Magnetic Fields in Semiconductor Physics II*, edited by G. Landwehr, Springer Series in Solid-State Sciences Vol. **87** (Springer-Verlag, Berlin 1989), p. 357.

FIG. 3. (a) Landau bands for  $s = 0.5$ .  $B_0 = 0.2$  T and  $a = 800$  nm, so that  $V_{\text{cyc}} = 0.85$  meV and  $\alpha = 0.041$  and (b) total magnetic field  $B(\xi_0)$ . The marked points on Landau bands 43 and 3 are the states for which the wave functions are shown in (c) and (d) in arbitrary units together with the corresponding effective potentials (dashed line). The wave functions are plotted with an offset, indicating the energy of the state. The states of (c) and (d) are to be compared with the classical orbits in Figs. 2 and 1 respectively.

FIG. 4. (a) Energy spectrum for  $s = 1$ .  $B_0 = 0.1$  T and  $a = 800$  nm, so that  $V_{\text{cyc}} = 0.21$  meV and  $\alpha = 0.17$ . The dashed lines show  $V(\xi_0, (2p+1)\pi)$  with  $|p| \leq 1$ . (b) Quantum mechanical (thick lines) and corresponding classical (thin lines) probability densities for two states. The chosen states are marked with dots in (a). (c) Effective potentials and classical orbits for  $E_F = 7V_{\text{cyc}}, \xi_0 = 0.5$  (solid lines) and  $E_F = 39.6V_{\text{cyc}}, \xi_0 = 3.18$  (dotted lines). The horizontal lines indicate the Fermi energy.

FIG. 5. (a): Effective potential  $V(\xi; \xi_0)$  for magnetic cosine modulation with  $s = B_m^0/B_0 = 2$ , and  $\xi_0/2\pi = 0.2$ . For given energy  $E_F$  (horizontal lines) classical orbits exist where  $V(\xi; \xi_0) \leq E_F$ . (b): Total magnetic field. (c): Locations of turning points  $\xi_0^\pm(\xi)$  for the  $E_F$  values indicated in (a). The outermost pair of lines belongs to the largest, the innermost pair to the smallest  $E_F$  value. The constant of motion  $\xi_0$  appears as a horizontal line in this plot ( $\xi_0/2\pi = 0.2$  is indicated). Orbits with fixed energy (i. e. fixed curves  $\xi_0^\pm(\xi)$ ) and this value of  $\xi_0$  exist in intervals with  $\xi_0^-(\xi) \leq \xi_0 \leq \xi_0^+(\xi)$ . Orbits, plotted in (d), with one turning point on  $\xi_0^-(\xi)$  and the other on  $\xi_0^+(\xi)$  are drifting orbits, the others are channeled orbits (see text).

FIG. 6. As in Fig. 5 but for  $s = 2$ , and  $\xi_0/2\pi = 0.5$ . Horizontal lines in (a) are for  $E_F/V_{\text{cyc}} = 40$  and  $E_F/V_{\text{cyc}} = 0.3$ . The inset shows  $V(\xi; \xi_0)$  enlarged between  $\xi = 0$  and  $\xi = 2\pi$ , where it has three zeroes. (c): For both indicated energies there exist three orbits, one drifting and two channeled orbits for  $E_F/V_{\text{cyc}} = 40$ , and three drifting orbits for  $E_F/V_{\text{cyc}} = 0.3$ , plotted in (d). Since the effective potential is symmetric, there is no guiding center drift for the central drifting orbits.

FIG. 7. (a) Energy spectrum (first 75 bands) for  $s = 2$ .  $B_0 = 0.05$  T and  $a = 800$  nm, so that  $V_{\text{cyc}} = 0.053$  meV and  $\alpha = 0.67$ . Effective potential and specific states (b) ( $n=0,20,22$ ) for  $\xi_0/2\pi = 0.5$  and (c) ( $n=0,1,2,25,44,45$ ) for  $\xi_0/2\pi = 0.2$ .

FIG. 8. (a) Energy spectrum (first 100 bands) for  $s = 2$ .  $B_0 = 0.2$  T and  $a = 800$  nm, so that  $V_{\text{cyc}} = 0.851$  meV and  $\alpha = 0.041$ . (c) Effective potential and specific states ( $n=0,2,3,4,5$ ), marked in extract of spectrum (b), for  $\xi_0/2\pi = 0.5$ .

FIG. 9. (a) Energy spectrum for  $s = 5$ ,  $B_0 = 0.1$  T and  $a = 800$  nm, so that  $V_{\text{cyc}} = 0.213$  meV and  $\alpha = 0.16$ . (b) Total magnetic field. (c) Effective potential and specific states for  $\xi_0/2\pi = 0.016$ . Typical channeled states  $n = 16$  and  $n = 22$  and a narrow drifting states,  $n = 19$ . (d) Effective potential and specific states for  $\xi_0/2\pi = 0.493$ . Wide drifting state,  $n = 17$ , narrow drifting states,  $n = 5$  and  $n = 6$ , and a channeled state,  $n = 7$ .

FIG. 10. Pure electric modulation of strength  $w = 20$ . (a) Energy spectrum (first 80 bands) for  $B_0 = 0.05$  T and  $a = 800$  nm, so that  $V_{\text{cyc}} = 0.053$  meV and  $\alpha = 0.67$ . (b) Drifting orbit (solid line) and channeled orbit (dotted line) for  $\xi_0/2\pi = 0.3$ . The energies (see marked states in (a)) are chosen in such a way, that  $\xi_c < \xi_0$  for the drifting and  $\xi_c > \xi_0$  for the channeled orbit, see text.

FIG. 11. (a) The first 175 Landau bands for combined magnetic and electric modulations.  $B_0 = 0.1$  T and  $a = 800$  nm, so that  $V_{\text{cyc}} = 0.213$  and  $\alpha = 0.16$ . The modulation strengths are  $s = 0.8$  and  $w = 14.3$ , the relative phaseshift is  $\pi/2$ . (b)  $\xi_0^\pm$ -curves for  $E/V_{\text{cyc}} = 110$ . At this energy  $\xi_0^+$  has local extrema, while there are none in  $\xi_0^-$ . Therefore all channeled orbits have negative velocities  $v_y$ .

Fig.1 Zwerschke

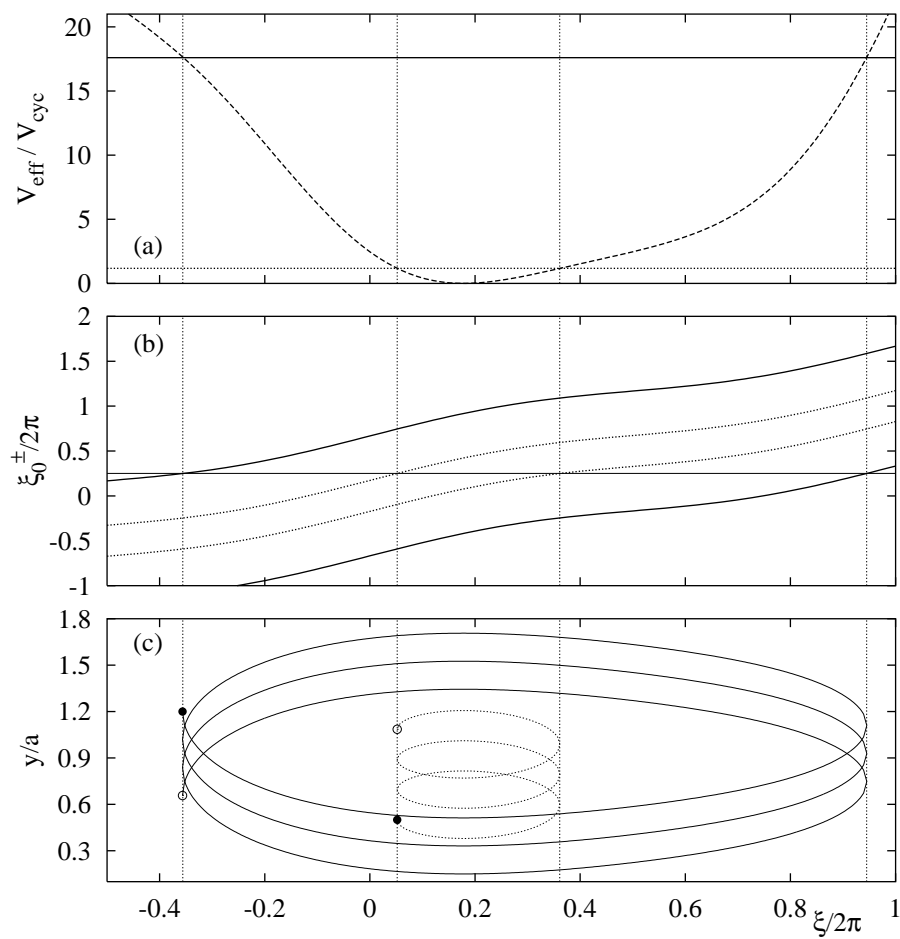


Fig.2 Zwerschke

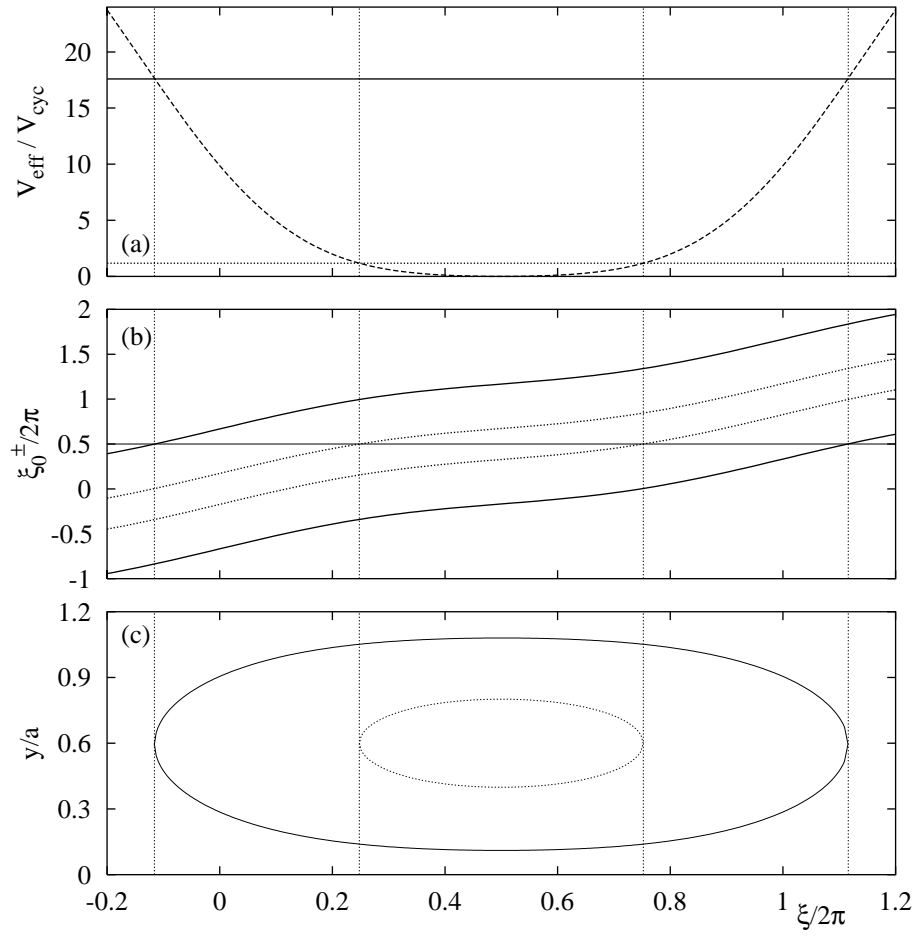


Fig.3 Zwerschke

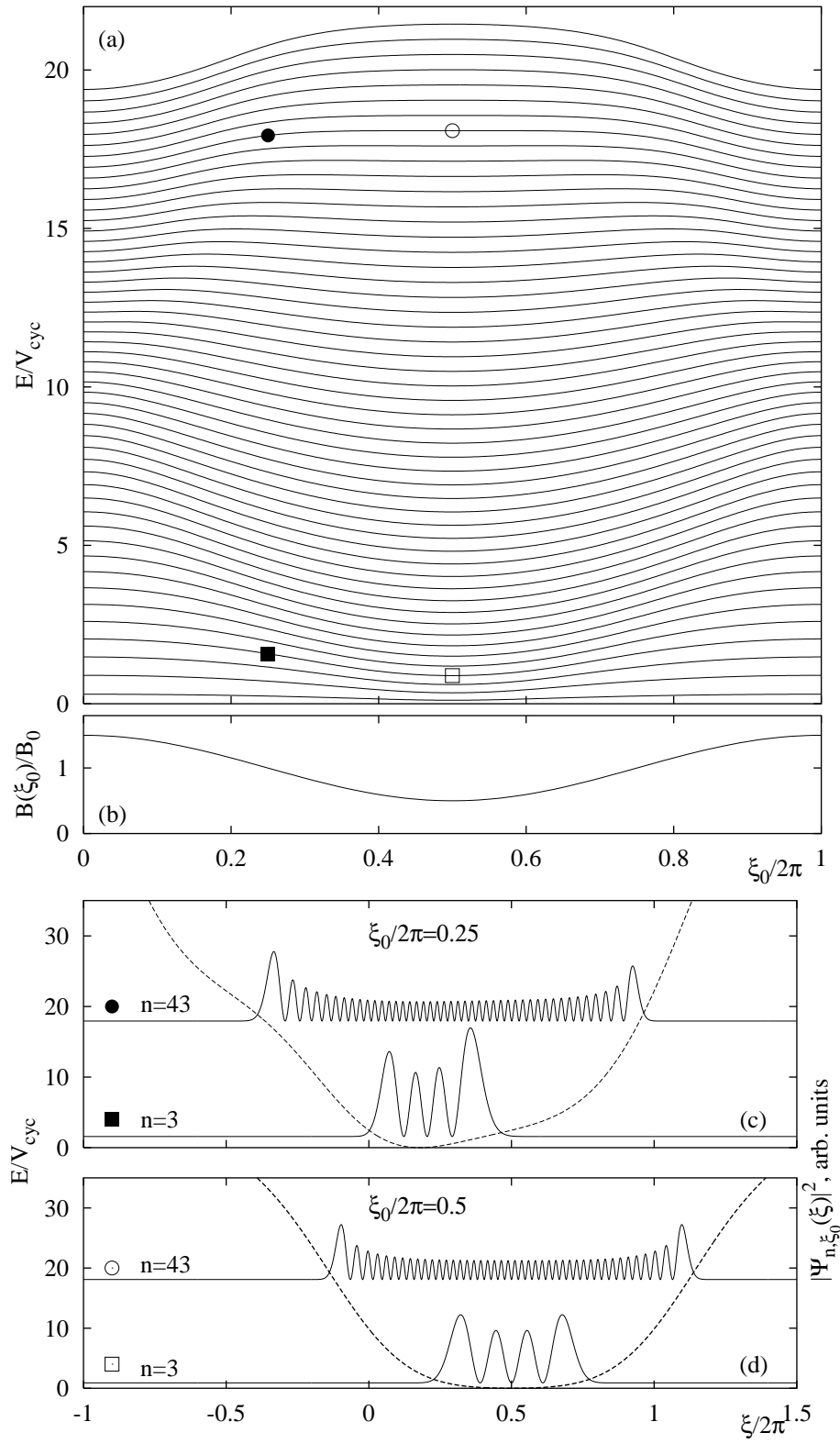


Fig.4 Zwerschke

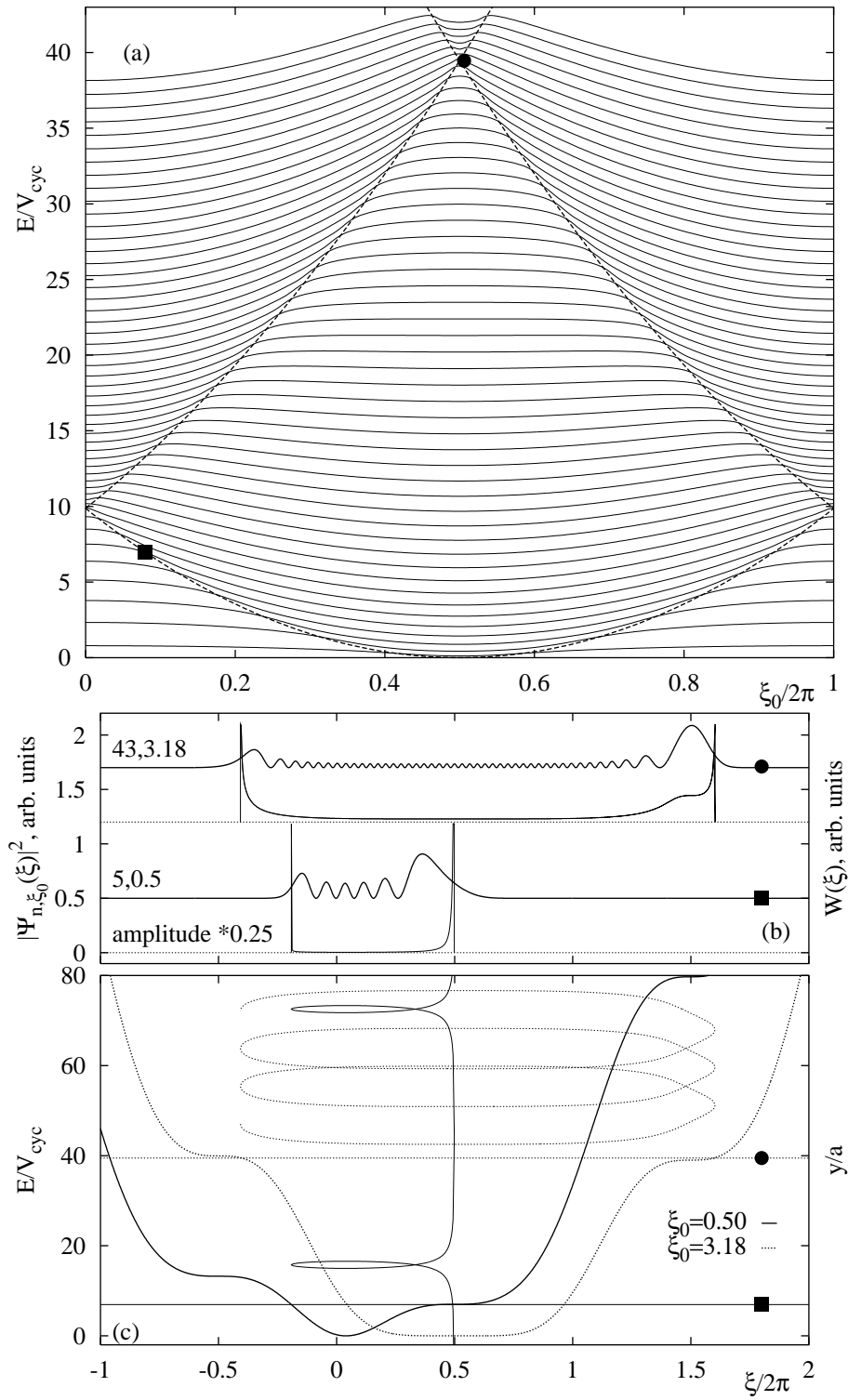


Fig.5 Zwerschke

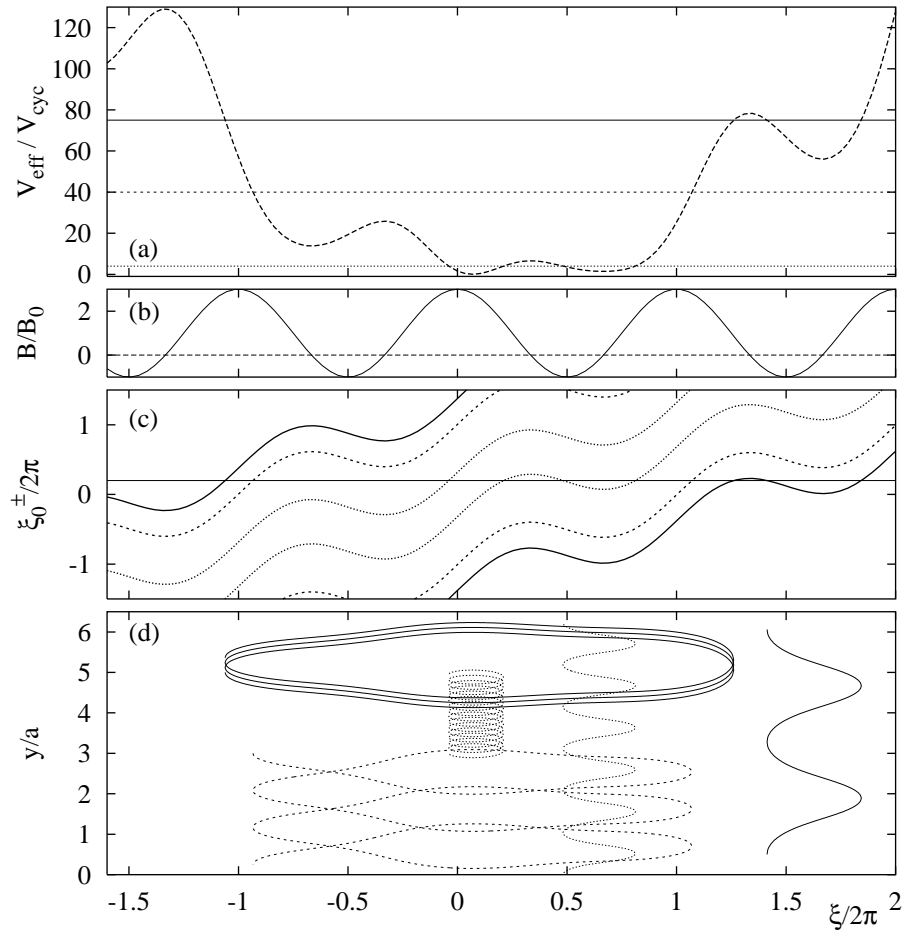




Fig.6 Zwerschke

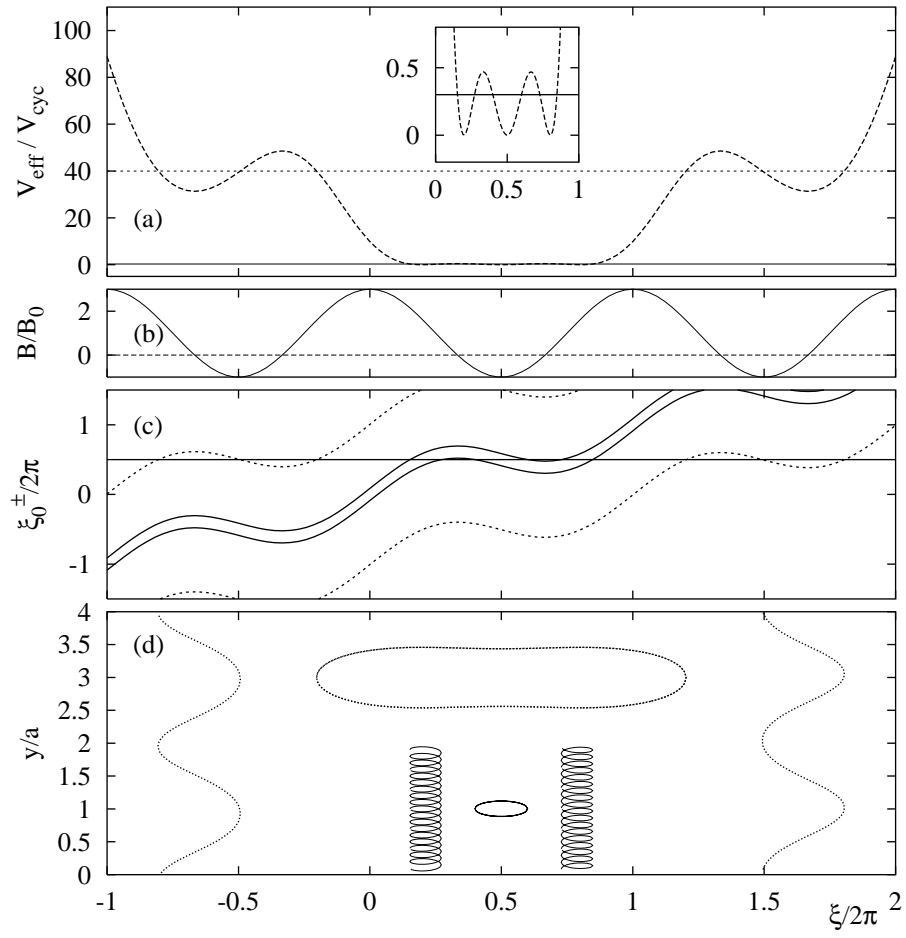


Fig.7 Zwerschke

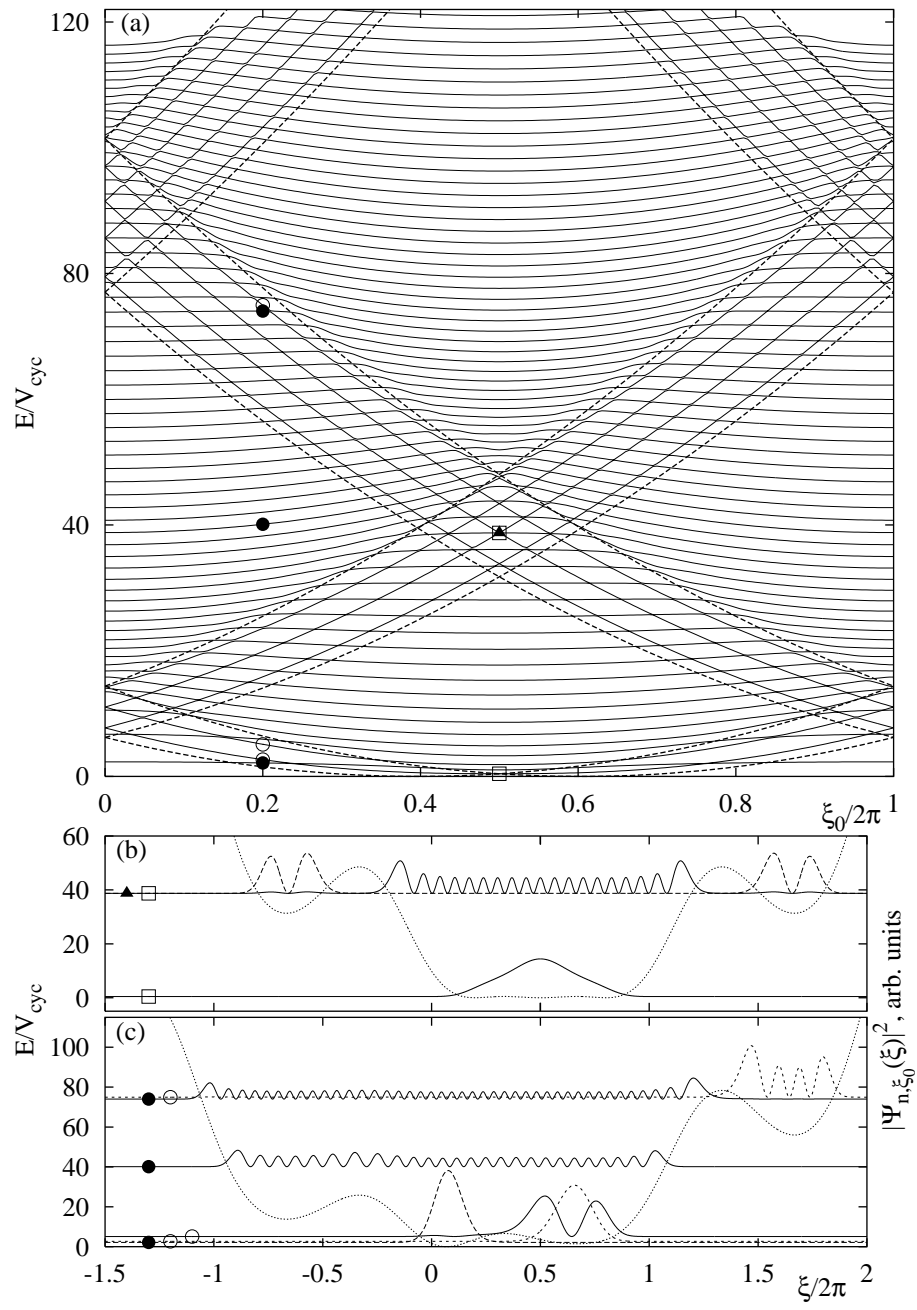


Fig.8 Zwerschke

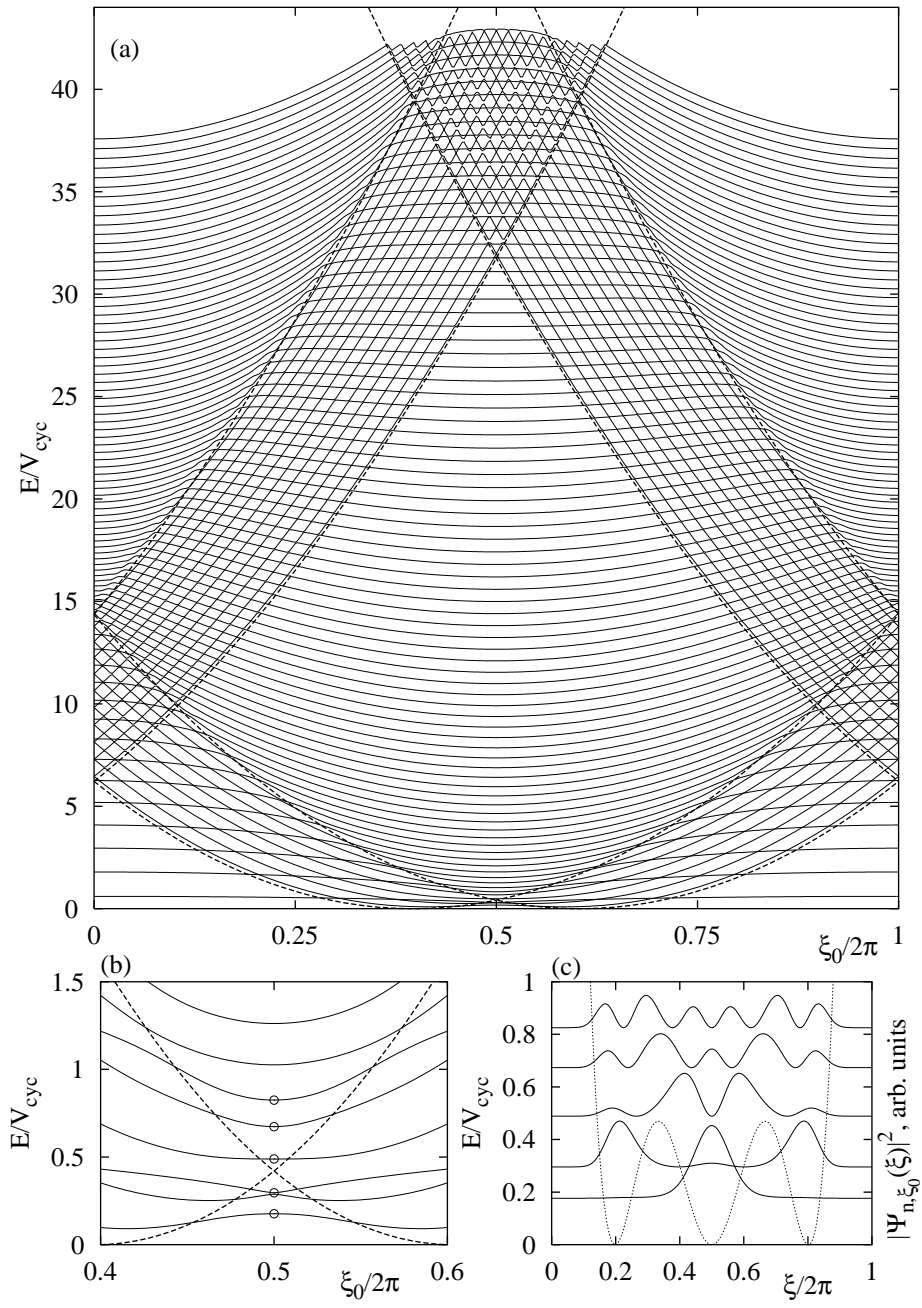


Fig.9 Zwerschke

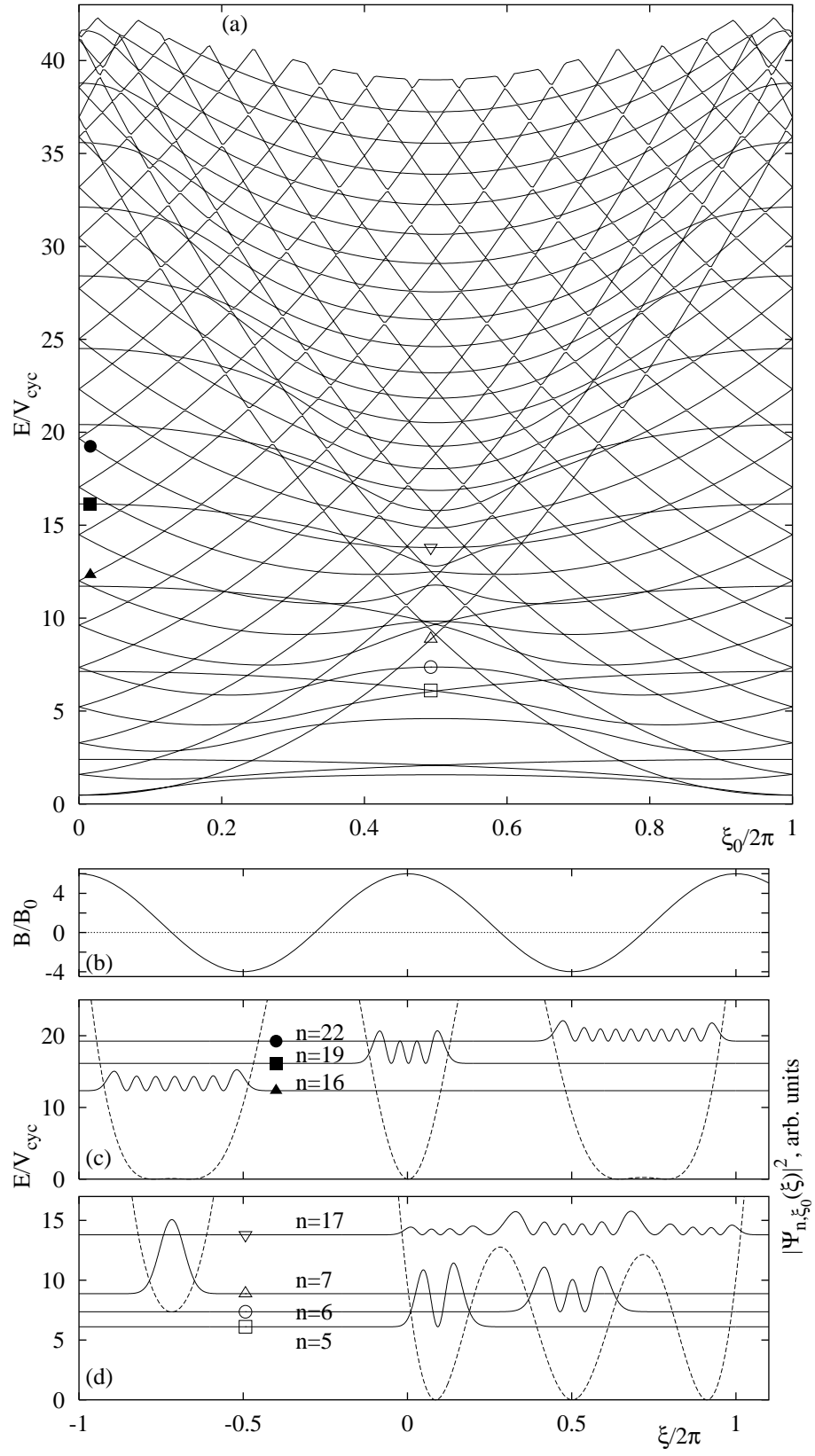


Fig.10 Zwerschke

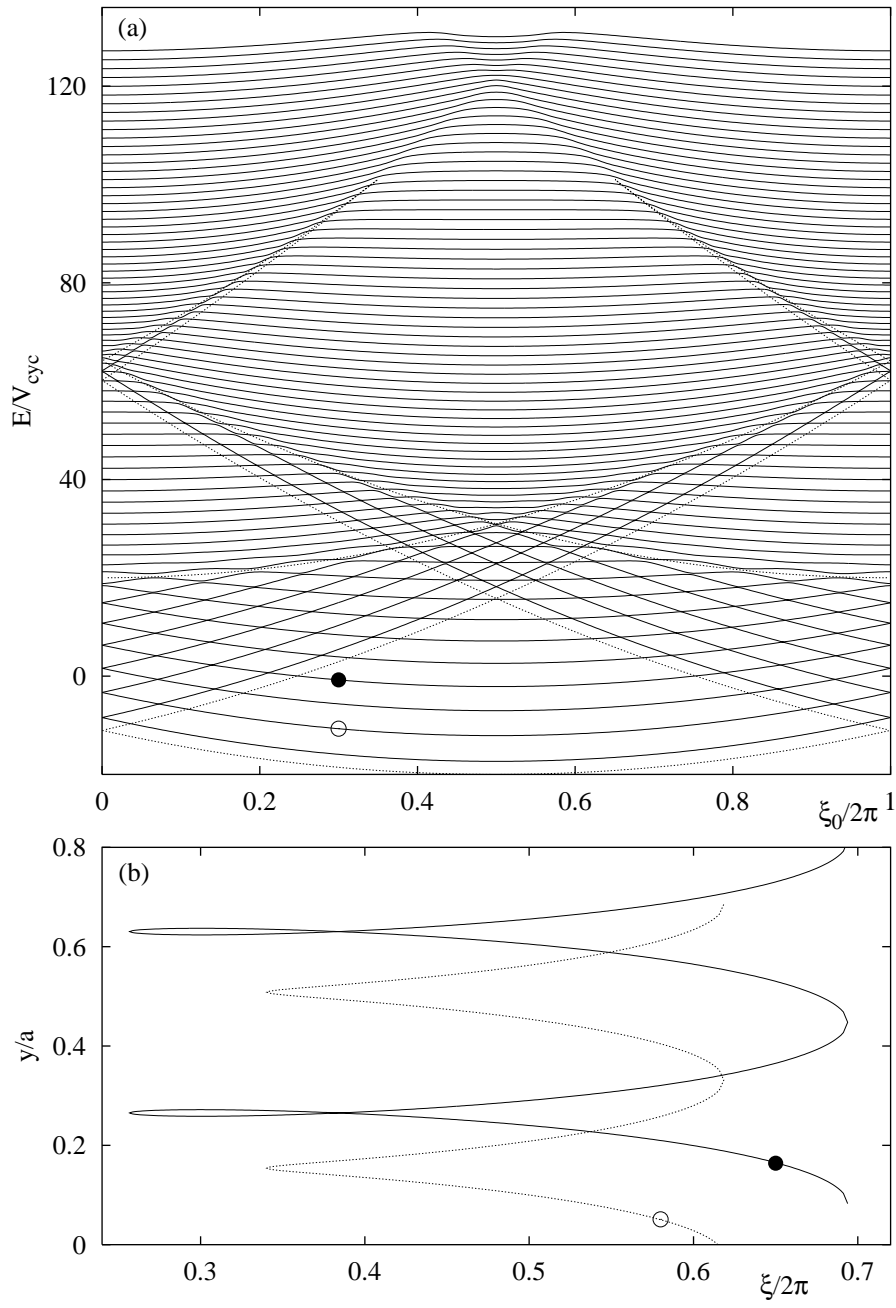


Fig.11 Zwerschke

